Monitoring the performances of a geosynthetic-reinforced pavement during construction

Danrong Wang[1*], *Sheng-Lin* Wang[1], *Susan* Tighe[2], *Sam* Bhat[3], and *Shunde* Yin[1]

[1]Department of Civil and Environmental Engineering, University of Waterloo, Waterloo, ON N2L 3G1, Canada
[2]Department of Civil Engineering, McMaster University, Hamilton, ON L8S 4L8, Canada
[3]Titan Environmental Containment Ltd., Ile des Chenes, MB R0A 0T1, Canada

Abstract. Geosynthetic materials have been widely used to enhance engineering practice in buildings, bridges, and pavements. As a kind of popular stabilization product, geogrid can be used for pavement reinforcement by serving as an additional tensile element. It has been demonstrated by many laboratory studies and numerical simulations that the reinforcement could significantly extend the fatigue life and improve the rutting resistance in flexible pavement. Meanwhile, geotextiles can provide soil separation, filtration and drainage; therefore, mitigating the freeze-thaw disturbances in the subgrade underneath the pavement structure. To study the application of geosynthetics in pavement structures in a more comprehensive aspect, a full-scale study was performed. A fibreglass geogrid which is specifically designed to reinforce the asphalt layer; as well as a geogrid composite material made of bi-axial geogrid bonded to a continuous filament non-woven geotextile, were installed in two field test sections. The geogrid was installed in the middle of the binder course within the asphalt layer, while the geogrid composite was placed at the interface of the base layer and subgrade in another section. The stiffness of the pavement was tested on each layer of the pavement structure during construction. As one of the major criteria to evaluate the pavement condition in North America, the International Roughness Index (IRI) was assessed to investigate the performances of geosynthetic-reinforced pavement during construction on asphalt binder course and surface course.

1 Introduction

Geosynthetic interlayers are widely applied with reinforcement, separation, and filtration to pavements. Laboratory testing results indicated that geogrid can extend the fatigue life of asphalt [1]. Crack propagation can also be inhibited by geogrid embedded in the asphalt [1]. Similar performances were also observed in several other studies by laboratory testing and modelling [2–4]. Geogrids have also been tested in large-scale field testing, demonstrating their capability to reduce pavement thickness while improving rutting resistance [5–7]. A cored pavement sample with geocomposite reinforcement was tested in the laboratory [8].

* Corresponding author: peggie.wang@uwaterloo.ca

Extensive studies were done to investigate the impact of geosynthetics on the pavements by laboratory testing and numerical modelling, while the monitoring of such reinforced pavements in real life during construction was not studied. This paper presents a full-scale field study with three trial sections in Ontario including geogrid composite installed on the subgrade and fibreglass geogrid embedded in the asphalt layer. Non-destructive test was performed during construction to monitor the impact of geosynthetic reinforcement on the pavement.

2 Methodology and Materials

The full-scale field study site was located in southern Ontario, Canada. The road has one lane in each direction and making up 45 m long in total for this study. Three trial sections, including one control section (CT) with conventional pavement structural design, one geogrid section (GG) with fibreglass geogrid embedded in the middle of the asphalt binder course, and one geogrid composite section (GC) with a geogrid composite material installed at the interface of granular base and subgrade, were constructed and studied. Each section is 15 m long. **Fig. 1** below illustrates the cross-sectional view for the trial sections and the location of the geosynthetics in the pavement structure.

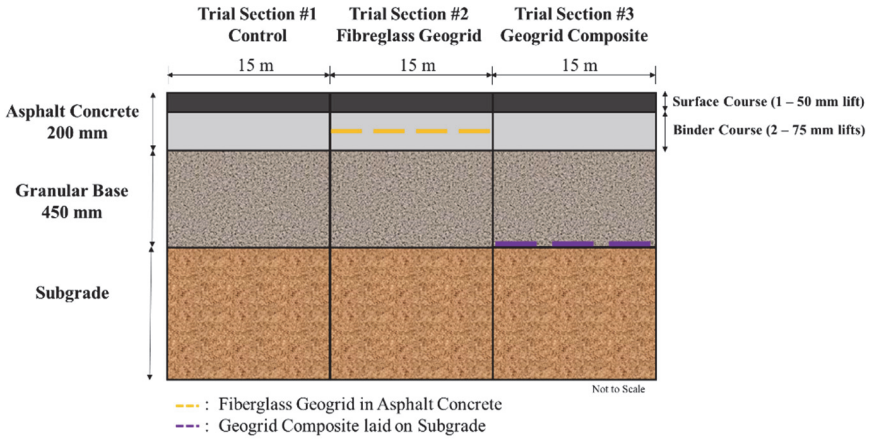

Fig. 1. Cross-Section View of Trial Sections

2.1 Materials

In the GG section, a biaxial fibreglass geogrid was installed between the two lifts of SP 19 asphalt binder courses. This product is manufactured from high-modulus glass filaments coated with a polymer [9]. The geogrid composite installed in the GC section comprises a biaxial polypropylene geogrid produced through a punching and drawing procedure, which is heat-bonded to a continuous filament non-woven polyester geotextile. [10]. The fibreglass geogrid and geogrid composite products are shown in **Fig. 2**. As depicted in Figure 1, the pavement structure consisted of an assembly comprising a 200 mm thick layer of asphalt concrete and a 450 mm thick granular base layer, above the subgrade, respectively. For all three sections, the base layer was established as an unbounded granular layer using Granular A. The asphalt concrete layer was constructed in three sequential lifts: from the top to the bottom, a 50 mm thick surface course using a Superpave (SP) 12.5 asphalt mix was applied, followed by two 75 mm thick binder course lifts using an SP 19 asphalt mix.

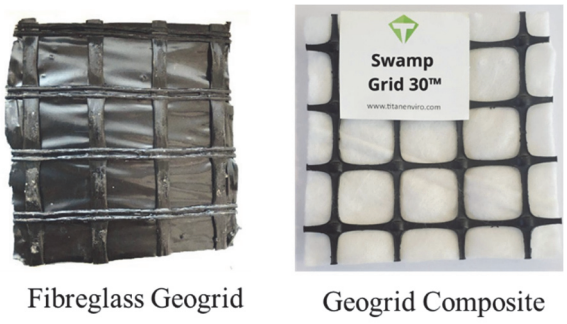

Fig. 2. Detailed View of Geosynthetic Materials

2.2 Light Weight Deflectometer

Light Weight Deflectometer (LWD) can be used to measure the deflection and stiffness of the subgrade, base, and pavement by releasing and applying loads on the layer. 15 kg weight is dropped from the height of 100 cm. The sudden drop of the weight can transmit the load to the ground, and the deflection can be used to calculate the stiffness. At least three consistent outcomes were ensured at one spot before moving to the next to obtain reliable measurements. 300 mm-diameter plate was used when performing the testing on the unbounded materials during construction. A 200 mm-diameter plate was used for the testing on the binder course and surface course as well as on the in-service pavement. Fig. 3 shows the LWD equipment.

Fig. 3. Light Weight Deflectometer (Left) and SurPro Equipment (Right)

2.3 SurPro

The SurPro walking profiler was used to measure the roughness of the pavements, including the paved binder course and surface course during construction and after construction, as shown in Fig. 3. The road was profiled by walking this equipment along both LWP and RWP on both lanes. The walking speed cannot exceed 2.5 m/s. The equipment was calibrated first before the testing by walking 50 m forward and 50 m reverse. The International Roughness Index (IRI) was generated, which is a commonly used standard indicator representing the roughness of a pavement.

3 Results

LWD was performed on the subgrade and base layer in the field during construction using a 300-mm diameter bearing plate. 200-mm diameter bearing plate was used on the asphalt binder course and surface course. LWD test was performed on the subgrade, base layer, asphalt binder course, and asphalt surface course. SurPro was run after the placement of the asphalt binder course and asphalt surface course.

3.1 Stiffness of Each Layer of Pavement Structure

3.1.1 Unbound Materials

During the construction, LWD was performed on the compacted subgrade, whose results are shown in Fig. 4. As it was indicated, the stiffness values of subgrade for the three sections were close to each other. Among them, subgrade in the GC section was the weakest.

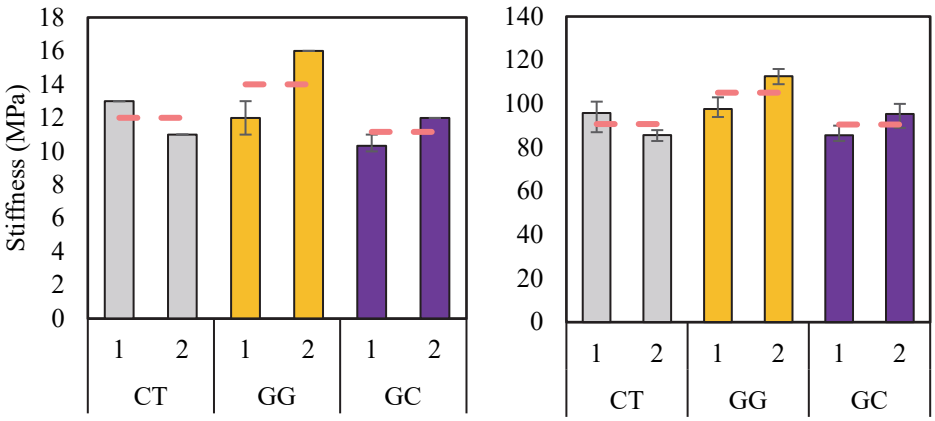

Fig. 4. LWD Tested Stiffness on Unbound Material on a) Subgrade; b) Base Layer

LWD was also performed on the compacted base layer, whose results of stiffness are shown in Fig. 4. With the weakest subgrade in the GC section, the stiffness tested on the base layer in the GC section was similar to that tested in the CT section after the geogrid composite and granular aggregate were placed. Overall, the stiffness conditions of the three sections were similar to each other on top of the subgrade and base layer, respectively.

3.1.2 Asphalt Layers

LWD test was performed on the asphalt binder course and asphalt surface course in the westbound lane, whose results are plotted in Fig. 5. The stiffness on the binder course is generally lower than that on the surface course, with the stiffness in the GC section showing a lower stiffness compared to the other two sections. This can be due to the weaker subgrade in the GC section as specified in the previous section. The effect of fibreglass geogrid within the asphalt was not obvious during the construction. However, after the traffic loading was applied, the effect may be more evident.

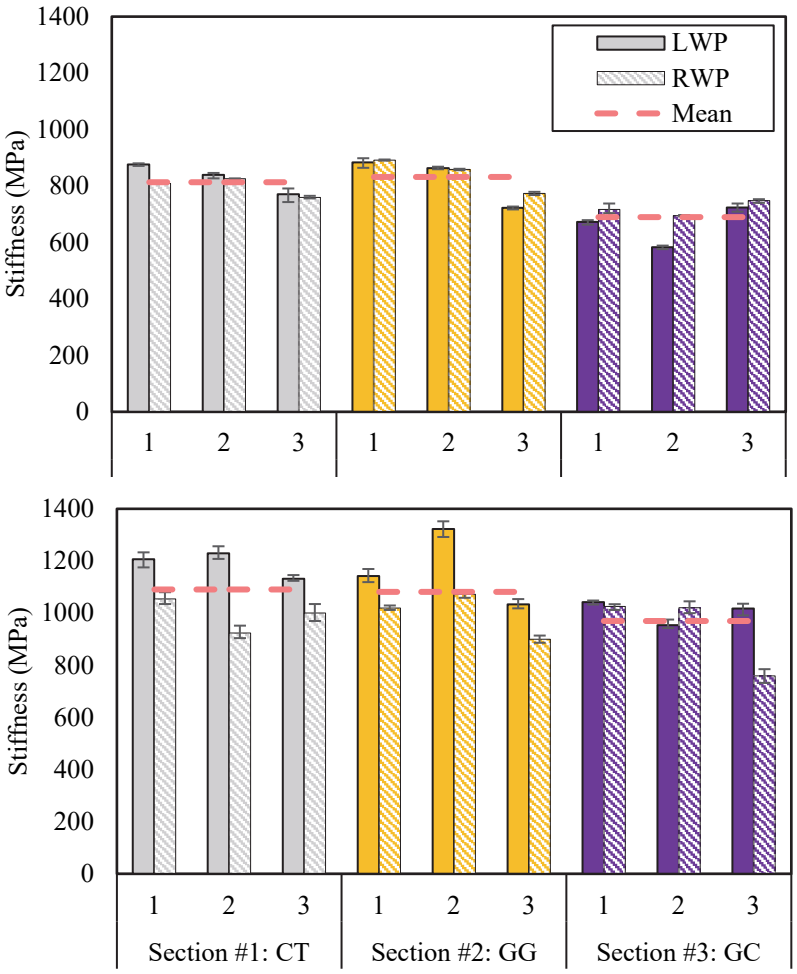

Fig. 5. LWD Tested Stiffness on Asphalt Binder Course (Top) and Surface Course (Bottom)

3.2 Roughness of Asphalt Layers

The roughness was measured using Surpro after the construction of the binder course and surface course. The IRI was calculated and analysed at every 1 m interval. The results tested after the binder course construction are shown in Fig. 6. One could see that, the highest IRI is shown in the geogrid section with an average of 3.96. On the other hand, the average IRI in the control section is 3.16, and the lowest IRI was measured at the geogrid composite section with an average of 2.34.

The results tested after the surface course construction are shown in Fig. 6, which shows a lower level of IRI compared to Fig. 6. The IRI values in the CT section and GG section were close, with an average of 2.35 and 2.29, respectively. The lowest IRI was still in the GC section with an average of 1.53.

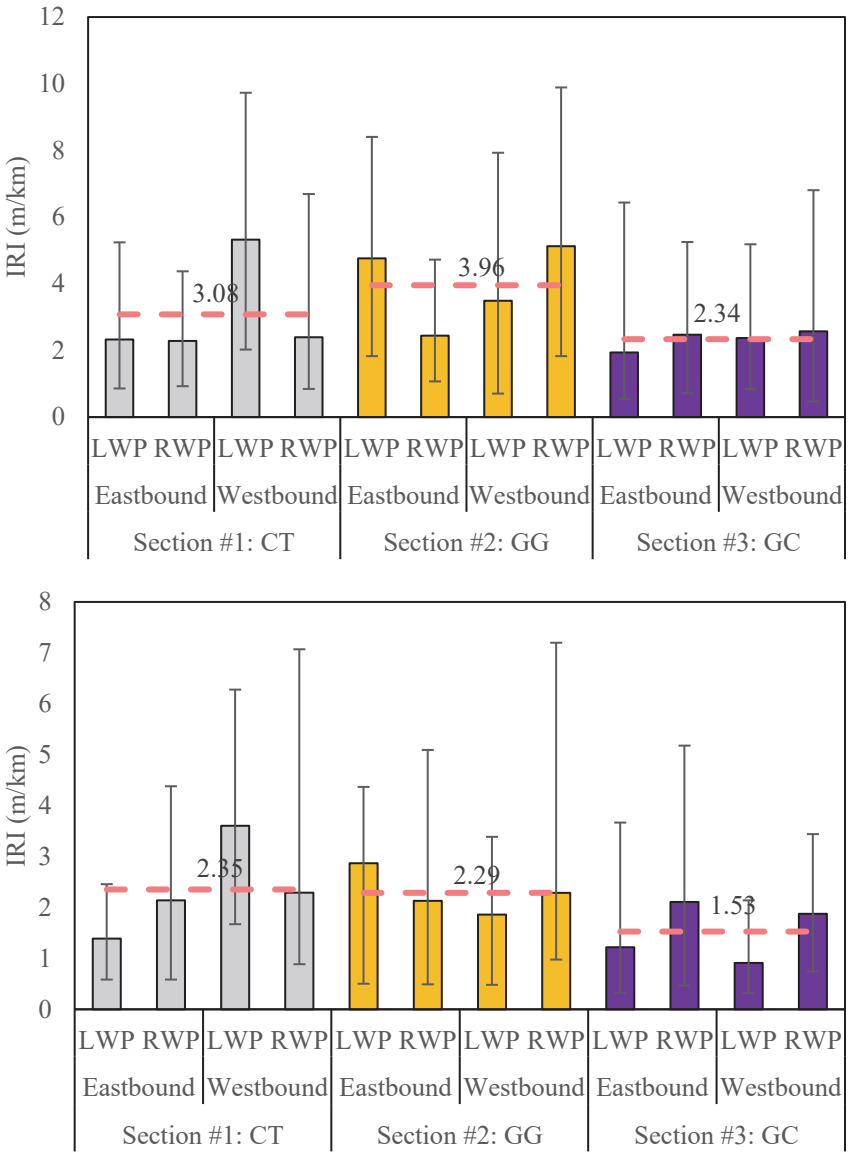

Fig. 6. IRI Results Tested after Placement of Binder Course (Top) and Surface Course (Bottom)

Despite the higher IRI on the binder course in the GG section, it appears that the roughness was reduced to the same level as that in the CT section after the surface course was paved. Therefore, an overlay of the surface course is necessary with the geogrid reinforcement in the asphalt concrete course. Additionally, the IRI measurements in the GC were shown to be the lowest on both the binder course and surface course, which implies a higher construction quality of asphalt. Compared with IRI measured after binder course placement, as plotted in Fig. 7, IRI generally dropped after surface course placement, which means the riding quality was improved. Among the three sections, the riding quality in the GG section improved the most. This concludes that an overlay is required to ensure the riding quality for pavement with geogrid embedded in the asphalt.

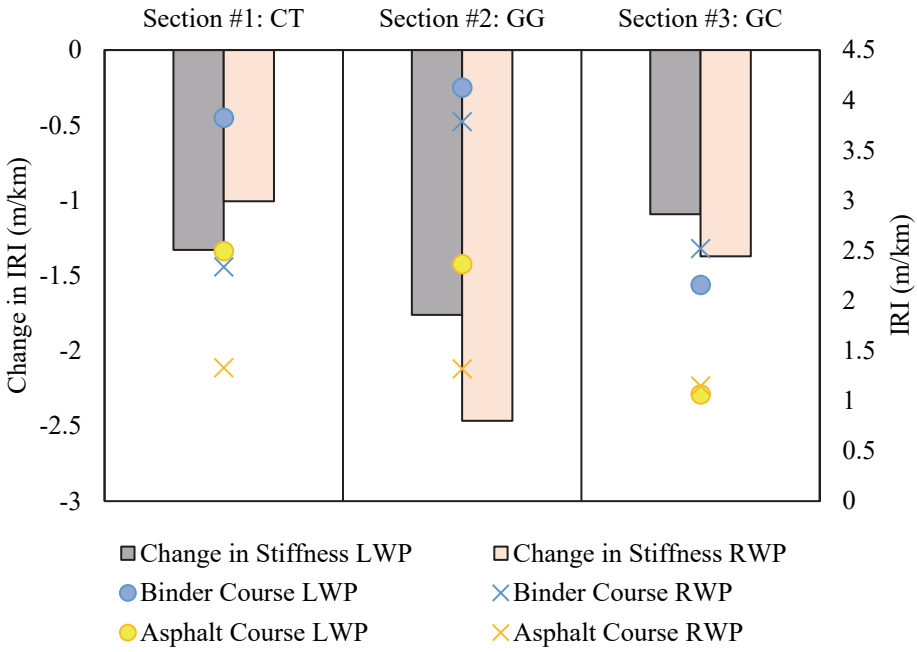

Fig. 7. Comparison of IRI on Binder Course and Surface Course

4 Conclusion

This paper presents the field testing performed on the trial sections in Ontario on geosynthetic-reinforced pavement. Non-destructive tests including LWD and SurPro were used to evaluate the pavement stiffness and roughness during construction.

The stiffness values of compacted subgrade, granular base, asphalt binder course, and asphalt surface course were tested separately. The unbound materials had similar structural capacity tested by LWD for the three sections. The stiffness was improved generally after the surface course was paved. A longer time is required for the effect of fibreglass geogrid embedded in the asphalt to show with more traffic loading applied. The significant reduction of IRI in the geogrid section was observed after the paving of surface course, which indicated the necessity of an additional surface overlay protection on top of the geogrid-reinforced asphalt concrete layer. Additionally, the IRI measurements in the geogrid composite were the lowest on both the binder course and surface.

In conclusion, the geogrid composite installed on the subgrade were proved to be able to provide reinforcement to weak subgrade with improved stiffness tested on granular base layer, as well as the lowest IRI on the asphalt surface. The effectiveness of the geogrid embedded in the asphalt need a longer term to be evident, while the construction quality was not affected by the geogrid within the asphalt with lower roughness after a surface overlay was applied.

References

1. S. J. Lee, Mechanical Performance and Crack Retardation Study of a Fiberglass-Grid-Reinforced Asphalt Concrete System, Canadian Journal of Civil Engineering **35**, 1042 (2008).

2. I. M. Arsenie, C. Chazallon, J. L. Duchez, and S. Mouhoubi, Modelling of the Fatigue Damage of a Geogrid-Reinforced Asphalt Concrete, Https://Doi.Org/10.1080/14680629.2016.1159973 **18**, 250 (2016).
3. T. Darzins, H. Qiu, and J. Xue, A Preliminary Laboratory Study of Fatigue Performance of Geogrid-Reinforced Asphalt Beam, Sustainable Civil Infrastructures 67 (2021).
4. V. V. Kumar, S. Saride, and J. G. Zornberg, Fatigue Performance of Geosynthetic-Reinforced Asphalt Layers, https://Doi.Org/10.1680/Jgein.21.00013 **28**, 584 (2021).
5. I. L. Al-Qadi, S. H. Dessouky, J. Kwon, and E. Tutumluer, Geogrid in Flexible Pavements Validated Mechanism, Transp Res Rec 102 (2008).
6. I. L. Al-Qadi, S. H. Dessouky, J. Kwon, and E. Tutumluer, Geogrid-Reinforced Low-Volume Flexible Pavements: Pavement Response and Geogrid Optimal Location, J Transp Eng **138**, 1083 (2012).
7. H. Alimohammadi, V. R. Schaefer, J. Zheng, and H. Li, Performance Evaluation of Geosynthetic Reinforced Flexible Pavement: A Review of Full-Scale Field Studies, International Journal of Pavement Research and Technology **14**, 30 (2021).
8. E. Pasquini, M. Pasetto, and F. Canestrari, Geocomposites against Reflective Cracking in Asphalt Pavements: Laboratory Simulation of a Field Application, Http://Dx.Doi.Org/10.1080/14680629.2015.1044558 **16**, 815 (2015).
9. Titan Environmental Containment, Spartan Road Grid TM 11EPM, 2017.
10. Titan Environmental Containment, Swamp Grid 30, 2021.